

Full Length Article

In situ electrical characterization of the Au/n-Si Schottky barrier structure under 1.2 MeV Ar ion irradiation

Jnaneswari Gellanki^a, Renu Kumari^b, Rekha Rani^b, Hemant Kumar Chourasiya^b, Sandeep Kumar^{b,*}^a Hansraj College, University of Delhi, Delhi 110 007, India^b Department of Physics, Central University of Rajasthan, Ajmer 305817, India

ARTICLE INFO

Keywords:

Energetic ions
Schottky Barrier diode
Electrical characteristics
Barrier height
Ion irradiation

ABSTRACT

Understanding the impact of energetic ion irradiation on semiconductor materials and devices is essential for optimizing their electronic applications. This knowledge contributes to the broader goal of tailoring material properties to enhance the overall performance and reliability of semiconductor devices. In this study, we investigate the impact of 1.2 MeV Ar⁸⁺ irradiation on Au/n-Si Schottky barrier structures in-situ, as a function of ion irradiation fluence. Electrical characterization was performed in-situ on a single sample to mitigate any variability in device parameters between samples. It is observed that ion irradiation results in an increased Schottky barrier height with a reduction in reverse leakage current. The behavior is attributed to dopant deactivation by the energetic ion irradiation-induced defects near the interface. These results underscore the importance of understanding ion irradiation impacts on semiconductor devices, providing valuable insights for optimizing Schottky diodes in electronic applications.

1. Introduction

The precise electrical characteristics of the metal–semiconductor (MS) contacts are the key requirement across diverse industries [1–4]. Effectively managing the properties at the MS interface emerges as a critical challenge during device fabrication. The reproducibility of these contacts is intricately linked to the surface preparation of the semiconductor and the annealing procedures after the metal contact deposition [5]. In the realm of metal/silicon contacts, the inherent SiO₂ and contaminants at the interface play significant roles. Even slight local variations in the structure of this oxide layer wield considerable influence over diode parameters [6]. The MS interface parameters like Schottky barrier height (SBH), extracted from electrical measurements, exhibit notable discrepancies from one diode to another, despite identical preparations [7,8]. To counteract these challenges, sintering is commonly employed, giving rise to interface states due to reactions at the interface. The non-uniform distribution of these interface states may induce an inhomogeneous barrier [9–11]. Therefore, there is a pressing need for reliable procedures to enhance control over the properties of Au/n-Si contacts. In this context, the exploration of energetic ion irradiation in semiconductors is actively pursued because energetic ions

have the potential to tailor the material properties in a controlled way [12–17]. Energetic ions can create deep-buried layers in materials with desired doping and controlled defects. While extensive research has been dedicated to modifying Schottky barriers (SBs) using ion beams [18–21], literature on the ion irradiation effect on SB structures at low irradiation fluences, particularly with ion energies within the vicinity of the MS interface, remains relatively scarce.

The SBH is one of the key parameters of an SBD, which intricately relies on the electric field at the MS interface [7,22]. This study is dedicated to the precise control of the SBD's barrier height by strategically managing the electric field at the MS interface. The study entails a meticulous in-situ current–voltage (I–V) characterization of Au/n-Si SBD during energetic ion irradiation at various ion fluences while maintaining constant physical parameters such as the vacuum environment, temperature, and measurement conditions. These findings not only advance our understanding of the intricate interplay between ion irradiation and Schottky structures but also provide valuable insights into tailoring their electrical properties.

* Corresponding author.

E-mail address: sandeep.kumar@curaj.ac.in (S. Kumar).<https://doi.org/10.1016/j.nimb.2024.165373>

Received 23 January 2024; Received in revised form 25 March 2024; Accepted 17 April 2024

Available online 22 April 2024

0168-583X/© 2024 Elsevier B.V. All rights reserved.

2. Experimental

The SBD were fabricated on n-type Si (100) substrates with a resistivity of 1.0–10 $\Omega\cdot\text{cm}$, purchased from MTI Corporation USA. A standard RCA cleaning process, involving a 10-minute boil in a solution of $\text{NH}_4\text{OH}/\text{H}_2\text{O}_2/\text{H}_2\text{O}$ (1:1:6), followed by a similar treatment in $\text{HCl}/\text{H}_2\text{O}_2/\text{H}_2\text{O}$ (1:1:6), was employed to eliminate surface contaminants. Subsequently, the wafer underwent deoxidization in 2 % hydrofluoric acid for 30 s, followed by rinsing in DI water with ultrasonic vibration and drying with high-purity nitrogen. Ohmic contacts were created on the cleaned Si wafer by depositing a 250 nm thick layer of aluminum via resistive heating, which was followed by annealing at 500 $^\circ\text{C}$ for 20 min in an argon gas atmosphere. For Schottky contacts, Au deposition was performed on the samples with Ohmic contacts using thermal resistive heating in a high vacuum chamber. The samples were cleaned (5 min in trichloroethylene, acetone and methanol sequentially) and deoxidized before making the Schottky contacts. A 100 nm Au layer was deposited through a stainless-steel mask with a contact diameter of 2 mm, at a base pressure of 10^{-6} mbar [9]. A schematic diagram of the device is shown in Fig. 1.

Ion irradiation was conducted using a 1.2 MeV Ar^{8+} beam at the Low Energy Ion Beam Facility (LEIBF) in the Inter-University Accelerator Centre, New Delhi [23]. The ion fluence ranged from 1×10^{10} to 1×10^{12} ions. cm^{-2} . This ion fluence range was chosen to minimize the occurrence of defect clustering, amorphization, enhanced sputtering, interface mixing, and structural damage. The average ionic current during irradiation was about 15 nA. The irradiation was performed at room temperature and there was no significant change in the sample temperature after ion irradiation. In-situ I-V characteristics of the SBDs were measured using a programmable Keithley 2400 source meter after stopping the ion beam at each fluence in a vacuum environment of approximately 10^{-7} mbar.

3. Results and discussion

Fig. 2 shows the I-V characteristics of the fabricated Au/n-Si SBD in forward bias, both before and after exposure to various ion irradiation fluences. A distinct linear region emerges at low forward biases (approximately 200 mV for the pristine sample), while higher voltage values manifest the predominant influence of the series resistance on the curve's behavior. Interestingly, it can be observed in Fig. 2 that with increasing ion irradiation fluence, the linear region shifts towards higher voltages (approximately 300 mV) after irradiation with 1×10^{12} ions. cm^{-2} . Simultaneously, there is a noticeable reduction in current within the region of series resistance at higher bias voltages. These insightful observations strongly suggest a simultaneous enhancement in both the SBH and series resistance of the diodes in response to ion irradiation, unraveling a dynamic aspect of their behavior under external influences.

The barrier parameters of the SBD, encompassing the ideality factor, SBH, ideality and series resistance, were meticulously calculated from Fig. 2 using the method pioneered by Cheung and Cheung [24]. This method, rooted in the principles of thermionic emission within a SBD structure incorporating series resistance, is elegantly expressed through Cheung's functions [24].

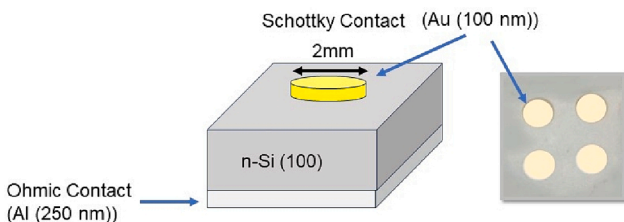


Fig. 1. A schematic diagram of Au/n-Si SBD.

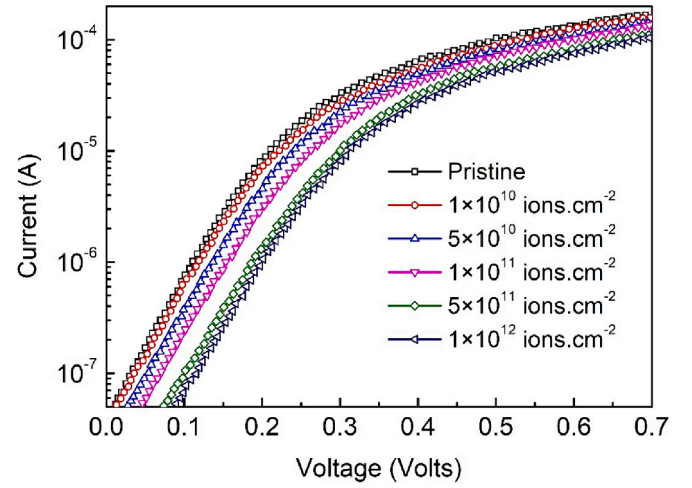


Fig. 2. Forward bias I-V characteristics of Au/n-Si SBD at various irradiation fluences.

$$\frac{dV}{d(\ln I)} = IR_s + n \left(\frac{kT}{q} \right) \quad (1)$$

$$H(I) = V - n \left(\frac{kT}{q} \right) \ln \left(\frac{I}{AA^*T^2} \right) \quad (2)$$

and

$$H(I) = IR_s + n\Phi_b \quad (3)$$

In these equations, IR_s represents the voltage drop across the series resistance (R_s) of the SBD. The symbol n denotes the ideality factor, k stands for the Boltzmann constant, A represents the contact area, A^* signifies the Richardson constant ($120 \text{ A/K}^2\text{cm}^2$ for n-Si), and Φ_b denotes the Schottky barrier height (SBH). Other symbols maintain their conventional meanings. Fig. 3(a) shows the plots of $dV/d(\ln I)$ vs. I and Fig. 3(b) shows the $H(I)$ vs. I plots at various ion irradiation fluences for the data of Fig. 2. For the data in the downward curvature region of Fig. 1, a straight line is obtained using Eq. (1). The analysis of $dV/d(\ln I)$ vs. I plots provides the series resistance as the slope and $n(kT/q)$ as the y-axis intercept [24]. Employing the n value derived from Eq. (2), a plot of $H(I)$ vs. I similarly result in a straight line, with the y-axis intercept equating to $n\Phi_b$. The slope of these plots furnishes a secondary determination of R_s , offering a mechanism to affirm the reliability and consistency of this analytical approach. The values of the extracted parameters are listed in Table 1.

For the pristine sample, the value of the ideality factor is 2.1, which increases to a value of 2.21 after exposure to an ion fluence of 1×10^{12} ions. cm^{-2} . It is observed that the value of the ideality factor remains relatively constant across the range of ion irradiation fluences used in this study. A high ideality factor typically suggests the presence of additional carrier transport mechanisms beyond thermionic emission. These additional mechanisms may include generation-recombination processes, trap-assisted tunneling, or interface states, which contribute to non-ideal behavior in the device [5,25]. The pristine diode showcased a barrier height of 0.74 eV. This relatively low barrier height is likely associated with the existence of a non-uniform thin oxide layer at the interface, associated with the device fabrication process. Ion irradiation induced a notable increase in the SBH, attaining a value of 0.80 eV after irradiation at a fluence of 1×10^{12} ions. cm^{-2} , as visually represented in Fig. 4. This increased SBH is accompanied by a simultaneous decrease in leakage current as depicted in Fig. 5. The leakage current exhibiting a reduction in value up to the highest fluence of 1×10^{12} ions. cm^{-2} . The observed increase in SBH and decrease in leakage current suggests a fundamental shift in the electrical properties of the MS interface.

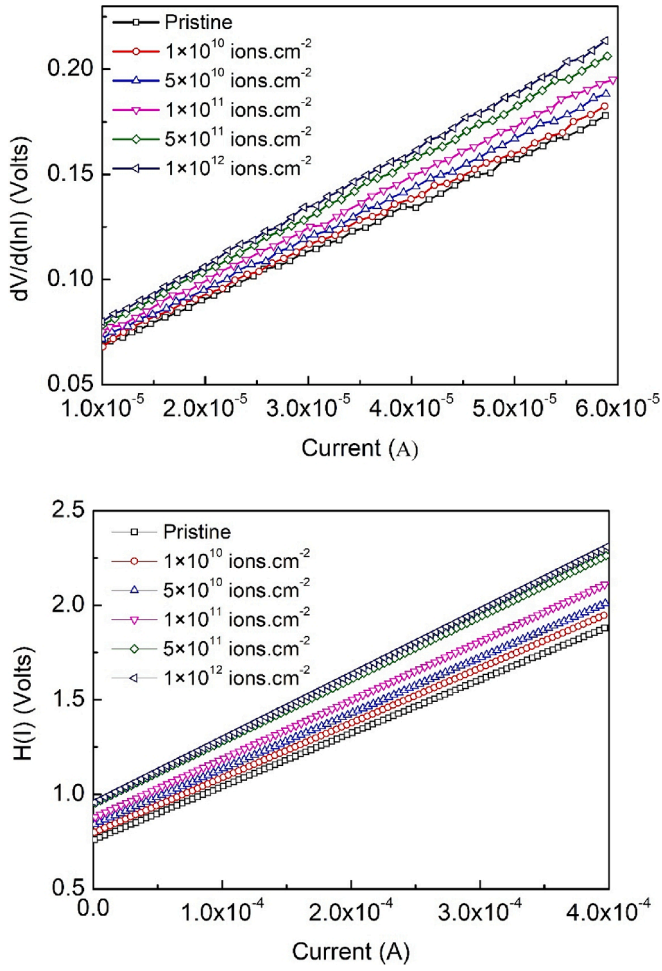


Fig. 3. (a) Plots of $dV/d(\ln I)$ vs. I , and (b) $H(I)$ vs. I for Au/n-Si SBD at different irradiation fluences.

Table 1

Irradiation fluence dependence of various parameters determined from forward bias I-V characteristics of Au/n-Si Schottky structure.

Fluence (ions. cm^{-2})	Ideality factor (n) (± 0.1)	Barrier height (± 0.01 (eV))	Resistance (dV/d ($\ln I$)-I) (± 0.02 (k Ω))	Resistance (H (I)-I) (± 0.02 (k Ω))
0	2.10	0.74	2.45	2.43
1×10^{10}	2.15	0.76	2.50	2.48
5×10^{10}	2.18	0.76	2.67	2.66
1×10^{11}	2.20	0.77	2.80	2.81
5×10^{11}	2.19	0.78	2.90	2.92
1×10^{12}	2.21	0.80	3.10	3.05

Additionally, an increase in series resistance was consistently noted across all irradiation fluences. As the resistance is inversely proportional to the product of mobility and carrier concentration, an increased value of resistance after ion irradiation indicates the value of carrier concentration and mobility is decreased [7,26]. When an energetic ion passes through a matter, it undergoes energy loss via elastic scattering by the target nuclei (nuclear energy loss, S_n) and inelastic interaction with the electrons (electronic energy loss, S_e). The energy loss of 1.2 MeV Ar^{8+} in Au/n-Si is depicted in Fig. 6. The incident ions traverse the MS interface and penetrate approximately $0.87 \mu\text{m}$ into the Si substrate. These calculations are performed using the standard Monte Carlo Simulation program SRIM 2015 [27]. The mean values of S_e and S_n at the MS interface are determined to be 1.25 keV/nm and 0.34 keV/nm,

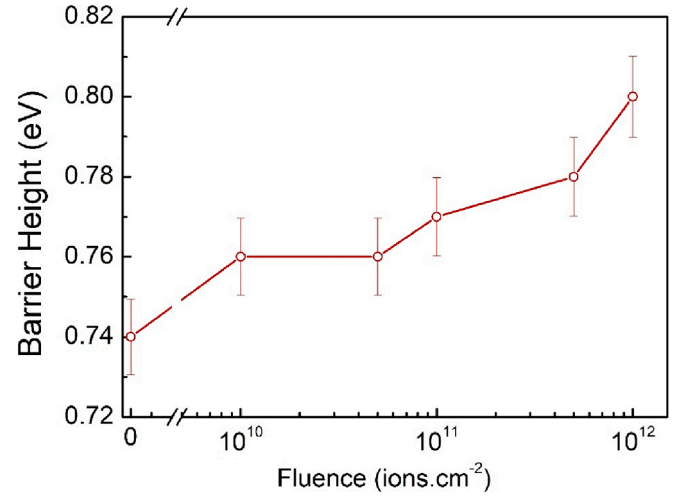


Fig. 4. Fluence dependence of the barrier height for the irradiated Au/n-Si Schottky barrier diode.

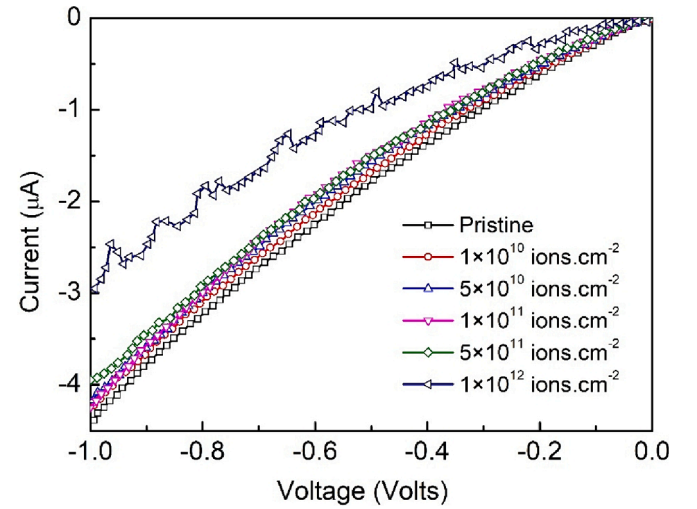


Fig. 5. Reverse bias current-voltage characteristics of Au/n-Si Schottky barrier diode at different irradiation fluences.

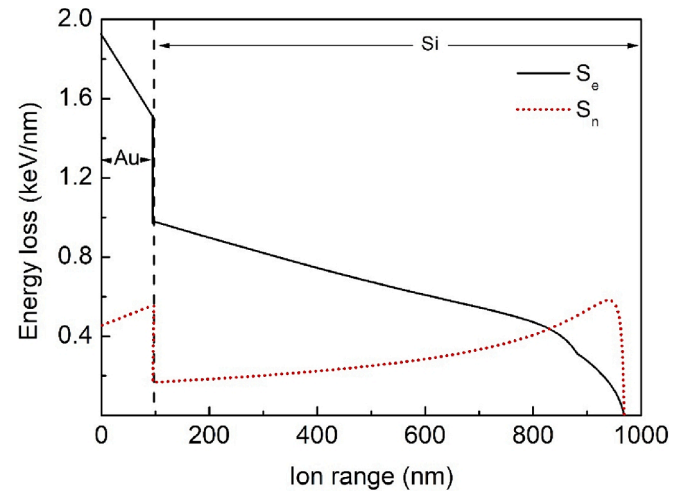


Fig. 6. Energy loss of 1.2 MeV Ar^{8+} in Au/n-Si SBD.

respectively. Nuclear energy loss leads to the displacement of target atoms, resulting in defects such as vacancies and interstitials, while electronic energy loss causes the excitation of target electrons. During the relaxation of these excited electrons, various types of defects may be generated. These defects can serve as scattering centers for carriers, reducing their mobility and consequently increasing the resistance.

Fig. 7 shows the capacitance–voltage characteristics ($1/C^2$ vs V) in the reverse bias of the SBD at different ion fluences. It is observed that the value of capacitance (C) decreases as the ion irradiation fluence increases. A decrease in the value of capacitance indicates a widening in the semiconductor depletion width. To maintain the charge neutrality condition at the interface, the widening of the depletion width arises due to a decrease in the concentration of ionized donors. Analysis of Fig. 6 shows that the carrier concentration decreases from a value of $4.7 \times 10^{15} \text{ cm}^{-3}$ for unirradiated SBD to $1.7 \times 10^{15} \text{ cm}^{-3}$ for SBD irradiated with $1 \times 10^{12} \text{ ions.cm}^{-2}$. The decrease in carrier concentration implies that ion irradiation induces defects with energy levels below the Fermi level in Au/n-Si SBD. These defects capture electrons from the conduction band, leading to a reduction in the equilibrium electron concentration. These defects also lead to the neutralization of positive shallow donors in the depletion region, altering the effective net ionized-donor concentration. The alteration in ionized donor concentration causes a variation in the thickness of the Schottky barrier. Consequently, dopant neutralization near the MS interface leads to an expansion of the thickness of the depletion region. A wider depletion region corresponds to a higher barrier height, which restricts the flow of minority carriers across the MS interface leading to a lower leakage current in reverse bias. The dopant deactivation after ion irradiation also changes the potential and electric field distribution in the interface region. The electric field at MS interface is given by [5]

$$E_{\max} = \frac{eN_D d}{\epsilon_s} \quad (4)$$

where d is the width of the depletion region, N_D is the dopant concentration and ϵ_s is the permittivity of the semiconductor. Since the image force lowering of the barrier depends on the square root of the maximum electric field ($\Delta\Phi_b = \left(\frac{qE_{\max}}{4\pi\epsilon_s}\right)^{1/2}$), a reduction in the electric field at the interface leads to an increase in the SBH. To summarize, the ideality factor exhibited negligible variation with irradiation fluence, while the SBH witnessed an increase, accompanied by a rise in series resistance. These observed changes are ascribed to dopant deactivation, the introduction of defects, and modifications in the electric field at the interface instigated by ion irradiation.

4. Conclusion

In conclusion, our investigation into the impact of ion irradiation on Au/n-Si Schottky barrier diodes revealed significant alterations in their electrical characteristics. The ideality factor exhibited limited variation across the ion irradiation fluences used. On the other hand, the Schottky barrier height displayed a notable increase, from a value of 0.74 eV for the pristine diode to 0.80 eV after irradiation at a fluence of $1 \times 10^{12} \text{ ions.cm}^{-2}$. This increase in barrier height was accompanied by a consistent decrease in the leakage current, indicating improved performance in reverse bias. The capacitance–voltage characteristics confirm that the fluence-dependent dopant deactivation near the metal–semiconductor interface played a crucial role in altering the electrical properties, contributing to an increased barrier thickness and a subsequent rise in Schottky barrier height. The consistent trends observed in our study underscore the importance of careful consideration of ion irradiation effects on semiconductor devices, offering valuable insights for the design and optimization of Schottky diodes in electronic applications. Further research in this direction could provide opportunities for tailoring material properties to enhance device performance and

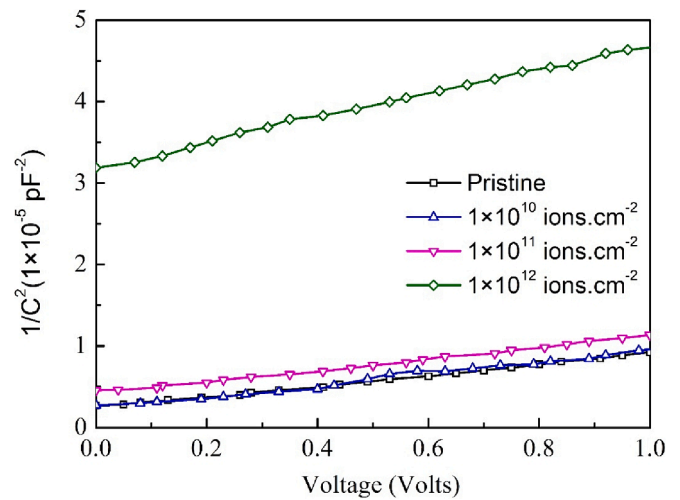


Fig. 7. Reverse bias $1/C^2$ vs V curve for Au/n-Si SBD at different ion fluences.

reliability.

CRediT authorship contribution statement

Jnaneswari Gellanki: Writing – original draft, Formal analysis, Data curation. **Renu Kumari:** Writing – review & editing, Formal analysis. **Rekha Rani:** Writing – review & editing, Formal analysis. **Hemant Kumar Chourasiya:** Writing – review & editing, Data curation. **Sandeep Kumar:** Writing – review & editing, Writing – original draft, Supervision, Project administration, Conceptualization.

Declaration of competing interest

The authors declare that they have no known competing financial interests or personal relationships that could have appeared to influence the work reported in this paper.

Data availability

Data will be made available on request.

Acknowledgements

The financial assistance through grant IUAC/XIII.7/UFR-70327 is highly acknowledged. The help received from P. Kumar during the experiment is gratefully acknowledged.

References

- [1] S.S. Chee, D. Seo, H. Kim, H. Jang, S. Lee, S.P. Moon, K.H. Lee, S.W. Kim, H. Choi, M.H. Ham, Lowering the Schottky Barrier Height by Graphene/Ag Electrodes for High-Mobility MoS₂ Field-Effect Transistors, *Adv. Mater.* 31 (2019) 1–7, <https://doi.org/10.1002/adma.201804422>.
- [2] P. Ji, S. Yang, Y. Wang, K. Li, Y. Wang, H. Suo, Y.T. Woldu, X. Wang, F. Wang, L. Zhang, Z. Jiang, High-performance photodetector based on an interface engineering-assisted graphene/silicon Schottky junction, *Microsyst. Nanoeng.* 8 (2022), <https://doi.org/10.1038/s41378-021-00332-4>.
- [3] I. Uddin, N.A.N. Phan, H.Y. Le Thi, H. Kim, D. Whang, G.H. Kim, MoTe₂-Based Schottky Barrier Photodiode Enabled by Contact Engineering, *ACS Appl. Nano Mater.* 6 (2023), <https://doi.org/10.1021/acsanm.2c04569>.
- [4] S. Gupta, A. Knoepfel, H. Zou, Y. Ding, Investigations of methane gas sensor based on biasing operation of n-ZnO nanorods/p-Si assembled diode and Pd functionalized Schottky junctions, *Sens. Actuata. B Chem.* 392 (2023), <https://doi.org/10.1016/j.snb.2023.134030>.
- [5] E.H. Rhoderick, R.H. Williams, *Metal-Semiconductor Contacts*, 2nd ed., Clarendon Press, Oxford, 1988.
- [6] H.K. Chourasiya, P.K. Kulriya, N. Panwar, S. Kumar, In-situ study of electrical transport in Pd/n-Si under high energy ion irradiation, *Semicond. Sci. Technol.* 35 (2020), <https://doi.org/10.1088/1361-6641/ab8e0d>.

- [7] S. Kumar, Y.S. Katharria, D. Kanjilal, Influence of 100 MeV oxygen ion irradiation on Ni/n-Si Schottky Barrier characteristics, *J. Appl. Phys.* 103 (2008) 21–23, <https://doi.org/10.1063/1.2885061>.
- [8] S. Kumar, Y.S. Katharria, D. Kanjilal, Influence of 100 MeV oxygen ion irradiation on Ni/n-Si (100) Schottky barrier characteristics, *J. Appl. Phys.* 103 (2008) 044504, <https://doi.org/10.1063/1.2885061>.
- [9] S. Kumar, Y.S. Katharria, V. Baranwal, Y. Batra, D. Kanjilal, Inhomogeneities in 130 MeV Au¹²⁺ ion irradiated Au/n-Si (1 0 0) Schottky structure, *Appl. Surf. Sci.* 254 (2008) 3277–3281, <https://doi.org/10.1016/J.APSUSC.2007.11.014>.
- [10] S. Neetika, A. Kumar, H.K. Sanger, A. Chourasiya, K. Kumar, R. Asokan, V. K. Chandra, Malik, Influence of barrier inhomogeneities on transport properties of Pt/MoS₂ Schottky barrier junction, *J. Alloy. Compd.* 797 (2019) 582–588, <https://doi.org/10.1016/j.jallcom.2019.05.028>.
- [11] J.H. Werner, H.H. Güttler, Barrier inhomogeneities at Schottky contacts, *J. Appl. Phys.* 69 (1991) 1522–1533, <https://doi.org/10.1063/1.347243>.
- [12] W. Paschoal, S. Kumar, C. Borschel, P. Wu, C.M. Canali, C. Ronning, L. Samuelson, H. Pettersson, Hopping conduction in Mn ion-implanted GaAs nanowires, *Nano Lett.* 12 (2012) 4838–4842, <https://doi.org/10.1021/nl302318f>.
- [13] S. Kumar, Y.S. Katharria, Y. Batra, D. Kanjilal, Influence of swift heavy ion irradiation on electrical characteristics of Au/n-Si (100) Schottky barrier structure, *J. Phys. D Appl. Phys.* 40 (2007) 6892–6897, <https://doi.org/10.1088/0022-3727/40/22/006>.
- [14] A.T. Sharma, S. Shahnawaz, Y.S. Kumar, D. Katharria, Kanjilal, Effects of swift heavy ion irradiation on the electrical characteristics of Au/n-GaAs Schottky diodes, *Appl. Surf. Sci.* 254 (2007) 459–463, <https://doi.org/10.1016/j.apsusc.2007.06.027>.
- [15] H.K. Chourasiya, P.K. Kulriya, N. Panwar, S. Kumar, Analysis of the carrier conduction mechanism in 100 MeV O⁷⁺ ion irradiated Ti/n-Si Schottky barrier structures, *Nucl. Instrum. Methods Phys. Res. B* 443 (2019) 43–47, <https://doi.org/10.1016/j.nimb.2019.01.045>.
- [16] S. Kumar, G.B. Correa Jr., C. Devi, A. Johannes, C. Ronning, W. Paraguassu, W. Paschoal Jr., H. Pettersson, D. Jacobsson, Evaluation of carrier density and mobility in Mn ion-implanted GaAs: Zn nanowires by Raman spectroscopy, *Nanotechnology* 31 (2020) 205705, <https://doi.org/10.1088/1361-6528/ab70fa>.
- [17] Y. Batra, D. Kabiraj, S. Kumar, D. Kanjilal, Ion-beam-induced phase separation in GeOx thin films, *J. Phys. D Appl. Phys.* 40 (2007), <https://doi.org/10.1088/0022-3727/40/15/029>.
- [18] S. Kumar, Y.S. Katharria, D. Kanjilal, Swift heavy ion irradiation-induced defects and electrical characteristics of Au/n-Si Schottky structure, *J. Phys. D Appl. Phys.* 41 (2008) 105105, <https://doi.org/10.1088/0022-3727/41/10/105105>.
- [19] M. Hua, Z. Xu, X. Tian, Z. Wang, C. Zhang, S. Zhao, Y. Zhang, J. Ning, Q. Feng, J. Zhang, H. Yue, Influence of swift heavy ion irradiation on electrical characteristics of β -Ga₂O₃ Schottky barrier diode, *Semicond. Sci. Technol.* 38 (2023), <https://doi.org/10.1088/1361-6641/acb45e>.
- [20] Y. Wang, M. Xiang, Y. Ma, M. Gong, R. Guo, M. He, X. Zhu, F. Mei, Y. Li, M. Huang, Z. Yang, J. Li, Z. Hu, Comparison of the effects of continuous and intermittent electron irradiation on commercial 4H-SiC Schottky barrier diodes, *Nucl. Instrum. Methods Phys. Res. B* 541 (2023), <https://doi.org/10.1016/j.nimb.2023.05.071>.
- [21] D.A. Oeba, J.O. Bodunrin, S.J. Moloi, Electrical properties of 3 MeV proton irradiated silicon Schottky diodes, *Phys. B Condens. Matter.* 610 (2021), <https://doi.org/10.1016/j.physb.2020.412786>.
- [22] Z.A. Jezeh, B. Efafi, B. Ghafary, The effect of electrode shape on Schottky barrier and electric field distribution of flexible ZnO photodiode, *Sci. Rep.* 11 (2021), <https://doi.org/10.1038/s41598-021-95203-3>.
- [23] D. Kanjilal, T. Madhu, G.O. Rodrigues, U.K. Rao, C.P. Savvan, A. Roy, Development of a low energy ion beam facility at NSC, *Indian J. Pure Appl. Phys.* 39 (2001).
- [24] S.K. Cheung, N.W. Cheung, Extraction of Schottky diode parameters from forward current-voltage characteristics, *Appl. Phys. Lett.* 49 (1986) 85–87, <https://doi.org/10.1063/1.97359>.
- [25] A. Arora, S. Mourya, N. Singh, S. Kumar, R. Chandra, V.K. Malik, Coexistence of Space Charge Limited and Variable Range Hopping Conduction Mechanism in Sputter-Deposited Au/SiC Metal-Semiconductor-Metal Device, *IEEE Trans. Electron Devices* 70 (2023) 714–719, <https://doi.org/10.1109/TED.2022.3232472>.
- [26] F. Roccaforte, S. Libertino, F. Giannazzo, C. Bongiorno, F. La Via, V. Raineri, Ion irradiation of inhomogeneous Schottky barriers on silicon carbide, *J. Appl. Phys.* 97 (2005) 123502, <https://doi.org/10.1063/1.1928328>.
- [27] James F. Ziegler, Jochen P. Biersack and Matthias D. Ziegler SRIM-The Stopping and Range of Ions in Matter, Pergamon, New York, 1985.